



CHORUS

This is the accepted manuscript made available via CHORUS. The article has been published as:

Imaging Molecular Motion: Femtosecond X-Ray Scattering of an Electrocyclic Chemical Reaction

M. P. Minitti, J. M. Budarz, A. Kirrander, J. S. Robinson, D. Ratner, T. J. Lane, D. Zhu, J. M. Glowia, M. Kozina, H. T. Lemke, M. Sikorski, Y. Feng, S. Nelson, K. Saita, B. Stankus, T. Northey, J. B. Hastings, and P. M. Weber

Phys. Rev. Lett. **114**, 255501 — Published 22 June 2015

DOI: [10.1103/PhysRevLett.114.255501](https://doi.org/10.1103/PhysRevLett.114.255501)

1 **Imaging Molecular Motion: Femtosecond X-Ray Scattering of an** 2 **Electrocyclic Chemical Reaction**

3
4 M.P. Minitti^{1*†}, J.M. Budarz^{1,2*}, A. Kirrander³, J.S. Robinson¹, D. Ratner¹, T.J. Lane^{1,4}, D. Zhu¹,
5 J.M. Glowacki¹, M. Kozina¹, H. T. Lemke¹, M. Sikorski¹, Y. Feng¹, S. Nelson¹, K. Saita³, B.
6 Stankus², T. Northey³, J.B. Hastings^{1†} & P.M. Weber^{2†}

7
8 *¹ SLAC National Accelerator Laboratory, Menlo Park, CA 94025 USA*

9 *² Brown University, Department of Chemistry, Providence, RI 02912 USA*

10 *³ School of Chemistry, University of Edinburgh, Edinburgh EH9 3JJ UK*

11 *⁴ Stanford University, Department of Chemistry, Stanford, CA 94305, USA*

12
13 **PACS Identifiers:** 61.05.cf, 33.15.-e and 41.60.Cr

14 **ABSTRACT**

15 Structural rearrangements within single molecules occur on ultrafast time scales.
16 Many aspects of molecular dynamics, such as the energy flow through excited states, have
17 been studied using spectroscopic techniques, yet the goal to watch molecules evolve their
18 geometrical structure in real-time remains challenging. By mapping nuclear motions using
19 femtosecond X-ray pulses, we have created real-space representations of the evolving
20 dynamics during a well-known chemical reaction and show a series of time-sorted
21 structural snapshots produced by ultrafast time-resolved hard X-ray scattering. A
22 computational analysis optimally matches the series of scattering patterns produced by the
23 X-rays to a multitude of potential reaction paths. In so doing we have made a critical step
24 toward the goal of viewing chemical reactions on femtosecond timescales, opening a new
25 direction in studies of ultrafast chemical reactions in the gas-phase.

26
* These authors contributed equally

† Corresponding authors: minitti@slac.stanford.edu, jbh@slac.stanford.edu and
Peter.Weber@brown.edu

27 **MAIN TEXT**

28
29 For more than a century, chemists have explored chemical reactions that transform
30 molecules from one structure to another. While mapping structure or function has become
31 routine in many instances, understanding the chemical dynamics that connect structure
32 and function remains, however, remarkably challenging [1]. A growing number of
33 experiments are emerging that aim to map chemical reactions with spatial and temporal
34 resolution, including molecular frame photoelectron spectroscopy [2], Coulomb explosion
35 imaging [3–5] and ultrafast electron diffraction [6]. It is notable that the most important
36 and frequently used techniques for the determination of static molecular structures,
37 namely x-ray scattering and nuclear magnetic resonance, are absent from this list.

38 X-ray scattering is one of the most powerful techniques for structure determination, but
39 the insufficient photon flux and too long pulse durations have rendered time-dependent
40 studies largely unfeasible. Some success has been attained using chopped x-ray pulses from
41 synchrotrons in the condensed phases for comparatively slow ($t \geq 50$ ps) chemical
42 processes [7,8]. Chemical reaction dynamics studies aimed at determining unique
43 structural conformations benefit from dilute gases where the reactions unfold uninhibited
44 by perturbations from neighboring molecules or collisions. Unfortunately the number of
45 molecules in the interaction region in many gas-phase samples are often too low to provide
46 sufficient signal with conventional x-ray sources, which also lack the time-resolution
47 required for reactions that unfold on the femtosecond time scale. Impressive advances
48 have been achieved using electron scattering [9–12]. Electron scattering has a qualitatively
49 larger cross-section than scattering of x-rays, but space-charge interactions between

50 electrons within a pulse make it difficult to reach the pulse durations needed to follow
51 molecular motions.

52 This paper demonstrates that x-ray scattering can be used as a tool to study gas-phase
53 ultrafast chemical reactions. The realization of hard x-ray free electron lasers (XFELs),
54 notably the Linac Coherent Light Source (LCLS) in 2009, has made available sources with
55 unprecedented x-ray brightness. Their pulse durations are as short as a few femtoseconds
56 and the intensity of a single x-ray pulse at LCLS is comparable to that available from
57 synchrotron sources integrated over one second. These parameters open up the possibility
58 to apply ultrafast x-ray sources to the study of chemical reaction dynamics in dilute
59 gases [13,14] and have now made it possible to observe molecular scattering patterns with
60 a time resolution approaching the ultrashort duration of laser pulses [15]. Scattering
61 experiments yield unique patterns that represent Fourier transforms of the molecular
62 structure. Because scattering experiments directly probe molecular geometry, they are
63 ideally suited for mechanistic studies on ultrafast time scales. We report here the first
64 observation of time-evolving x-ray scattering patterns from dilute gas phase molecules
65 during a chemical reaction: the ultrafast ring-opening reaction of 1,3-cyclohexadiene (CHD)
66 to form linear 1,3,5-hexatriene (HT).

67 The ring-opening reaction of CHD has intrigued scientists for many years. As a
68 prototypical example of an electrocyclic reaction, it has played an important role in the
69 understanding of a large class of organic reactions [16]. The reaction motif also features
70 prominently in synthetic processes, photochemical switches, and natural product
71 synthesis [17]. Upon excitation by a UV photon, the molecule slides down the potential
72 energy surface of the $1B$ electronic state and goes through a conical intersection to reach a

73 steeply repulsive 2A surface, from where it transitions via an avoided crossing to the
74 ground state of the reaction product [17]. From spectroscopic experiments, the time scales
75 are known [18–20] but the correlation of time constants to molecular structures has
76 remained absent. By applying x-ray scattering we are now able to assign molecular
77 structures to each time point of the reaction before the molecules reach a thermal
78 equilibrium of conformational structures [21].

79 The experiment was performed at the X-ray Pump-Probe (XPP) Instrument of
80 LCLS [22]. Briefly, CHD vapor at a pressure of 3-4 Torr, corresponding to only $\sim 1 \cdot 10^{17}$
81 molecules/cm³, for a total of $\sim 8 \cdot 10^{12}$ total molecules in the interaction region, were
82 introduced into a custom scattering chamber, Fig. 1. The ring-opening reaction was
83 initiated by the absorption of a 267 nm optical pump photon (65 fs, 4-8 μ J, 100 μ m FWHM
84 focus). The structural evolution of CHD to HT was observed by a time-delayed x-ray probe
85 (8.3 keV, 30 fs, 10^{12} photons/pulse, 30 x 30 μ m FWHM focus) propagating collinearly with
86 the pump laser. Scattering patterns were collected on a 2.3-megapixel CSPAD imaging
87 detector [23] as a function of time delay. For each pump-probe pair, precise relative arrival
88 times of the x-ray and optical pulses at the sample were monitored by a spectrally-encoded
89 cross-correlator [24,25]. Fast data collection enabled the adjustment of experimental
90 parameters, such as delay time and beam overlap, to optimize experimental conditions
91 during the experimental runs.

92 The percentage changes in the measured scattering signal for momentum transfers
93 between 1.0 and 4.2 \AA^{-1} as a function of delay between optical laser excitation and the x-ray
94 probe are shown in Fig 2. The changes are on the order of 1%, which we estimate
95 corresponds to an average of 7% of the molecules excited by the pump pulse. In the

96 experiment, the percentage of molecules excited was deliberately kept low to minimize
97 multiphoton processes. Immediately after optical excitation, the difference scattering signal
98 appears as either positive or negative changes as a function of momentum transfer and
99 time delay. No further changes were observed after approximately 200 fs. This is consistent
100 with optical pump-probe experiments that have suggested that the molecule evolves on the
101 excited electronic state surfaces for about 140 fs [14].

102 The time dependence of the scattering signal for specific momentum transfers is
103 shown in Fig. 3A. The analysis (Fig. 3B & 3C) shows that certain momentum transfers are
104 associated with transient features as short-lived as 75 fs while others have considerably
105 longer lifetimes. The difference in the observed rates and lifetimes for various regions of
106 momentum transfer (Fig. 3B & 3C) are simply attributed to the distances between non-
107 neighboring carbons within CHD/HT moving with respect to one another on different
108 timescales. The shortest lived transients (Fig. 3B) exhibit lifetimes on the order of the
109 dissociation reaction [14], suggesting that the experiment captures the CHD molecule as it
110 reacts in the time domain.

111 The x-ray scattering results show that the structural part of the transformation of 1,3-
112 cyclohexadiene to 1,3,5-hexatriene proceeds with an 80 fs time constant. This compares
113 with the decay (140 fs) of the last electronic state populated in the reaction sequence and
114 the point from where hexatriene is generated (the $2A$ surface), as reported from
115 spectroscopic experiments [17]. The time scale also compares with a 30 fs lifetime of the
116 initially excited $1B$ electronic state, and the separately observed spectroscopic appearance
117 time of structurally disperse hexatriene of 140 fs [26]. The x-ray scattering experiment
118 presented here, solely limited by the achievable momentum vector resolution, not only

119 provides reliable time constants for the structural evolution of the reaction, but also allows
120 one to calculate representative molecular structures along the reaction path consistent
121 with the experiment.

122 To determine the time-evolution of molecular structure implied by the experimental
123 data we start by calculating 100 trajectories, which represent a wide range of plausible
124 reaction paths. Each trajectory is obtained with slightly different starting conditions
125 sampled from a vibrational Wigner distribution of the $v=0$ vibrational state of the S_0
126 electronic ground state [27]. Trajectories are propagated using the multiconfigurational
127 Ehrenfest method [28] with potential energies and non-adiabatic couplings obtained *on-*
128 *the-fly* from SA3-CAS(6,4)-SCF/cc-pVDZ *ab initio* electronic structure calculations using
129 Molpro [29]. The all-atom simulations do not assume any reduced representation or pre-
130 existing reaction coordinate. Three electronic states are included: the ground state, the
131 optically accessed *1B* state, and the *2A* state that is implicated in the Woodward-Hoffman
132 mechanism of the electrocyclic reaction [16]. The rotationally averaged coherent scattering
133 signal is obtained via the independent-atom model by [30]

$$134 \quad I(t, q) = \sum_i^{N_{atom}} |f_i^0(q)|^2 + \sum_{i \neq j}^{N_{atom}} f_i^0(q) f_j^0(q) \frac{\sin q R_{ij}(t)}{q R_{ij}(t)} \quad (1)$$

135 using published elastic scattering atomic form factors [31], $f_i^0(q)$, and internuclear
136 distances, $R_{ij}(t)$, taken from our trajectories. Each trajectory constitutes a molecular
137 reaction path with a complete but distinct set of interatomic distances. For visualization, it
138 is helpful to represent the trajectories in terms of a single distance, that between the
139 terminal carbons C1 and C6 in HT, which corresponds to the bond that breaks in CHD
140 during the reaction. While all trajectories start near the 1.54 Å bond distance of CHD [17],

141 the trajectories diverge within the first 50 fs of the reaction, as can be seen in
142 Supplementary Figure 1. Some of the molecules remain initially in bonded form, but open
143 up after one or more oscillations.

144 To determine the combination of trajectories that best describes the chemical reaction,
145 we compare the experimental scattering patterns with scattering patterns calculated from
146 the computed trajectories. Using a multi-start nonlinear least-square optimization routine
147 with a finite-difference gradient [32], we determined the weights on the trajectories which
148 result in a signal that best matches the experimental data in Fig. 2. The optimization
149 converges on a small number of trajectories (highlighted in Supplementary Figure 2) with
150 the four dominant trajectories having a combined weight of approximately 80%, and the
151 remaining 20% made up by four more trajectories. Based on the representation of x-ray
152 scattering embodied by equation (1), these trajectories suffice to represent the
153 experimentally observed data, within the approximations inherent in equation (1) and a
154 classical representation of the chemical reaction. A direct comparison of the theoretical
155 signal and the experimental data at particular time points is shown in Fig. 4. Movies
156 showing the time-evolving molecular structures of the four dominant trajectories (bold
157 lines in Supplementary Figure 2) are available as extended data (Supplementary Movies 1-
158 4).

159 Our analysis shows that upon absorption of the optical photon, the chemical reaction
160 of 1,3-cyclohexadiene to 1,3,5-hexatriene starts with a rapid expansion of the carbon bonds
161 of the cyclohexadiene ring. This expansion is related to the weakening of the chemical
162 bonds due to the electronic excitation of the molecular π -bonds. Within one or two
163 oscillations of the carbon skeleton, the C1-C6 chemical bond breaks as the terminal carbon

164 atoms move perpendicular to the molecular plane along the reaction coordinate. It is
165 already at this point that the terminal hydrogen atoms of the nascent hexatriene molecule
166 align to conform to the Woodward-Hoffman rules [16]. Consequently, the stereochemical
167 fate of the chemical reaction is sealed as early as thirty femtoseconds after the optical
168 excitation.

169 In summary, we report the first ultrafast time-resolved gas-phase x-ray scattering
170 experiment, recording the ring-opening reaction of 1,3-cyclohexadiene using femtosecond
171 hard x-ray pulses from LCLS, and thereby opening a new direction for time-resolved x-ray
172 scattering experiments for chemical dynamics. Time-dependent x-ray scattering patterns
173 from molecular structures as they evolve during chemical reactions can provide important
174 feedback to mechanistic studies, as well as to computational methods that aim to elucidate
175 chemical reaction mechanisms. Such data should prove quite useful to spectroscopic
176 experiments, which associate specific spectral features with time points in the reaction.
177 With the time-evolution of molecular structure available from x-ray scattering experiments,
178 the spectroscopic results can be better matched to computer simulations, providing
179 synergy between different experimental techniques and theory. In particular, important
180 spectroscopic experiments that explore the path of the molecule through the conical
181 intersections can now be coupled with structural information. The time-dependent
182 molecular structures during the electrocyclic ring-opening reaction of 1,3-cyclohexadiene
183 to 1,3,5-hexatriene obtained in the present work will help form an important foundation
184 for a significant body of future XFEL experimental and computational studies. We
185 anticipate an exciting period of rapid developments in ultrafast x-ray scattering
186 experiments that push both temporal and spatial resolution boundaries, as well as in the

187 theoretical and computational framework required to interpret these new experiments.

188 REFERENCES

- 189 [1] A. H. Zewail, *J. Phys. Chem. A* **104**, 5660 (2000).
- 190 [2] P. Hockett, C. Z. Bisgaard, O. J. Clarkin, and A. Stolow, *Nat. Phys.* **7**, 612 (2011).
- 191 [3] H. Ibrahim, B. Wales, S. Beaulieu, B. E. Schmidt, N. Thiré, E. P. Fowe, É. Bisson, C. T.
192 Hebeisen, V. Wanie, M. Giguère, J.-C. Kieffer, M. Spanner, A. D. Bandrauk, J. Sanderson,
193 M. S. Schuurman, and F. Légaré, *Nat. Commun.* **5**, 4422 (2014).
- 194 [4] J. L. Hansen, J. H. Nielsen, C. B. Madsen, A. T. Lindhardt, M. P. Johansson, T. Skrydstrup,
195 L. B. Madsen, and H. Stapelfeldt, *J. Chem. Phys.* **136**, 204310 (2012).
- 196 [5] L. Christensen, J. H. Nielsen, C. B. Brandt, C. B. Madsen, L. B. Madsen, C. S. Slater, A.
197 Lauer, M. Brouard, M. P. Johansson, B. Shepperson, and H. Stapelfeldt, *Phys. Rev. Lett.*
198 **113**, 073005 (2014).
- 199 [6] C. J. Hensley, J. Yang, and M. Centurion, *Phys. Rev. Lett.* **109**, 133202 (2012).
- 200 [7] H. Ihee, M. Lorenc, T. K. Kim, Q. Y. Kong, M. Cammarata, J. H. Lee, S. Bratos, and M.
201 Wulff, *Science* **309**, 1223 (2005).
- 202 [8] R. Neutze, R. Wouts, S. Techert, J. Davidsson, M. Kocsis, A. Kirrander, F. Schotte, and M.
203 Wulff, *Phys. Rev. Lett.* **87**, 195508 (2001).
- 204 [9] R. C. Dudek and P. M. Weber, *J. Phys. Chem. A* **105**, 4167 (2001).
- 205 [10] J. B. Hastings, F. M. Rudakov, D. H. Dowell, J. F. Schmerge, J. D. Cardoza, J. M. Castro, S.
206 M. Gierman, H. Loos, and P. M. Weber, *Appl. Phys. Lett.* **89**, 184109 (2006).
- 207 [11] H. Ihee, V. A. Lobastov, U. M. Gomez, B. M. Goodson, R. Srinivasan, C. Y. Ruan, and a H.
208 Zewail, *Science* **291**, 458 (2001).
- 209 [12] B. J. Siwick, J. R. Dwyer, R. E. Jordan, and R. J. D. Miller, *Science* **302**, 1382 (2003).
- 210 [13] J. Küpper, S. Stern, L. Holmegaard, F. Filsinger, A. Rouzée, A. Rudenko, P. Johnsson, A.
211 V. Martin, M. Adolph, A. Aquila, S. Bajt, A. Barty, C. Bostedt, J. Bozek, C. Caleman, R.
212 Coffee, N. Coppola, T. Delmas, S. Epp, B. Erk, L. Foucar, T. Gorkhover, L. Gumprecht, A.
213 Hartmann, R. Hartmann, G. Hauser, P. Holl, A. Hömke, N. Kimmel, F. Krasniqi, K.-U.
214 Kühnel, J. Maurer, M. Messerschmidt, R. Moshhammer, C. Reich, B. Rudek, R. Santra, I.
215 Schlichting, C. Schmidt, S. Schorb, J. Schulz, H. Soltau, J. C. H. Spence, D. Starodub, L.
216 Strüder, J. Thøgersen, M. J. J. Vrakking, G. Weidenspointner, T. a. White, C. Wunderer,

- 217 G. Meijer, J. Ullrich, H. Stapelfeldt, D. Rolles, and H. N. Chapman, *Phys. Rev. Lett.* **112**,
218 083002 (2014).
- 219 [14] V. S. Petrović, M. Siano, J. L. White, N. Berrah, C. Bostedt, J. D. Bozek, D. Broege, M.
220 Chalfin, R. N. Coffee, J. Cryan, L. Fang, J. P. Farrell, L. J. Frasinski, J. M. Glowina, M. Gühr,
221 M. Hoener, D. M. P. Holland, J. Kim, J. P. Marangos, T. Martinez, B. K. McFarland, R. S.
222 Minns, S. Miyabe, S. Schorb, R. J. Sension, L. S. Spector, R. Squibb, H. Tao, J. G.
223 Underwood, and P. H. Bucksbaum, *Phys. Rev. Lett.* **108**, 253006 (2012).
- 224 [15] P. Emma, R. Akre, J. Arthur, R. Bionta, C. Bostedt, J. Bozek, A. Brachmann, P.
225 Bucksbaum, R. Coffee, F.-J. Decker, Y. Ding, D. Dowell, S. Edstrom, A. Fisher, J. Frisch, S.
226 Gilevich, J. Hastings, G. Hays, P. Hering, Z. Huang, R. Iverson, H. Loos, M.
227 Messerschmidt, A. Miahnahri, S. Moeller, H.-D. Nuhn, G. Pile, D. Ratner, J. Rzepiela, D.
228 Schultz, T. Smith, P. Stefan, H. Tompkins, J. Turner, J. Welch, W. White, J. Wu, G. Yocky,
229 and J. Galayda, *Nat. Photonics* **4**, 641 (2010).
- 230 [16] B. Woodward, A. Press, B. S. House, B. Square, and T. C. Society, *Angew. Chem. Int. Ed.*
231 *Engl.* **8**, 781 (1969).
- 232 [17] S. Deb and P. M. Weber, *Annu. Rev. Phys. Chem.* **62**, 19 (2011).
- 233 [18] M. Garavelli, C. S. Page, P. Celani, M. Olivucci, W. E. Schmid, S. A. Trushin, and W. Fuss,
234 *J. Phys. Chem. A* **105**, 4458 (2001).
- 235 [19] N. Kuthirummal, F. M. Rudakov, C. L. Evans, and P. M. Weber, *J. Chem. Phys.* **125**,
236 133307 (2006).
- 237 [20] K. Kosma, S. A. Trushin, W. Fuss, and W. E. Schmid, *Phys. Chem. Chem. Phys.* **11**, 172
238 (2009).
- 239 [21] C. Y. Ruan, V. A. Lobastov, R. Srinivasan, B. M. Goodson, H. Ihee, and a H. Zewail, *Proc.*
240 *Natl. Acad. Sci. U. S. A.* **98**, 7117 (2001).
- 241 [22] S. Moeller, J. Arthur, A. Brachmann, R. Coffee, F.-J. Decker, Y. Ding, D. Dowell, S.
242 Edstrom, P. Emma, Y. Feng, A. Fisher, J. Frisch, J. Galayda, S. Gilevich, J. Hastings, G.
243 Hays, P. Hering, Z. Huang, R. Iverson, J. Krzywinski, S. Lewis, H. Loos, M.
244 Messerschmidt, A. Miahnahri, H.-D. Nuhn, D. Ratner, J. Rzepiela, D. Schultz, T. Smith, P.
245 Stefan, H. Tompkins, J. Turner, J. Welch, B. White, J. Wu, G. Yocky, R. Bionta, E. Ables, B.
246 Abraham, C. Gardener, K. Fong, S. Friedrich, S. Hau-Riege, K. Kishiyama, T. McCarville,
247 D. McMahon, M. McKernan, L. Ott, M. Pivovarov, J. Robinson, D. Ryutov, S. Shen, R.
248 Soufli, and G. Pile, *Nucl. Instruments Methods Phys. Res. Sect. A Accel. Spectrometers,*
249 *Detect. Assoc. Equip.* **635**, S6 (2011).
- 250 [23] H. T. Philipp, M. Hromalik, M. Tate, L. Koerner, and S. M. Gruner, *Nucl. Instruments*
251 *Methods Phys. Res. Sect. A Accel. Spectrometers, Detect. Assoc. Equip.* **649**, 67 (2011).

- 252 [24] M. R. Bionta, H. T. Lemke, J. P. Cryan, J. M. Glowonia, C. Bostedt, M. Cammarata, J.-C.
253 Castagna, Y. Ding, D. M. Fritz, a R. Fry, J. Krzywinski, M. Messerschmidt, S. Schorb, M.
254 L. Swiggers, and R. N. Coffee, *Opt. Express* **19**, 21855 (2011).
- 255 [25] M. Harmand, R. Coffee, M. R. Bionta, M. Chollet, D. French, D. Zhu, D. M. Fritz, H. T.
256 Lemke, N. Medvedev, B. Ziaja, S. Toleikis, and M. Cammarata, *Nat. Photonics* **7**, 215
257 (2013).
- 258 [26] C. C. Pemberton, Y. Zhang, and P. M. Weber, (n.d.).
- 259 [27] R. C. Brown and E. J. Heller, *J. Chem. Phys.* **75**, 186 (1981).
- 260 [28] K. Saita and D. V Shalashilin, *J. Chem. Phys.* **137**, 22A506 (2012).
- 261 [29] MOLPRO, version 2012.1, a package of ab initio programs (2012).
- 262 [30] P. Debye, *Ann. Phys.* **351**, 809 (1915).
- 263 [31] A. Wilson, *International Tables for Crystallography, Vol. C, Mathematical, Physical, and*
264 *Chemical Tables* (Kluwer Academic Publishers, Dordrecht/Boston/London, 1995), pp.
265 475–536.
- 266 [32] M. P. Minitti, J. M. Budarz, A. Kirrander, J. Robinson, T. J. Lane, D. Ratner, K. Saita, T.
267 Northey, B. Stankus, V. Cofer-Shabica, J. Hastings, and P. M. Weber, *Faraday Discuss.*
268 **171**, 81 (2014).
- 269 [33] See Supplemental Material [url], which includes Refs. [34-47].
- 270 [34] S. Herrmann, P. Hart, A. Dragone, D. Freytag, R. Herbst, J. Pines, M. Weaver, G. a Carini,
271 J. B. Thayer, O. Shawn, C. J. Kenney, and G. Haller, *J. Phys. Conf. Ser.* **493**, 012013
272 (2014).
- 273 [35] U. Lorenz, K. B. Møller, and N. E. Henriksen, *New J. Phys.* **12**, 113022 (2010).
- 274 [36] R. Srinivasan, V. A. Lobastov, C.-Y. Ruan, and A. H. Zewail, *Helv. Chim. Acta* **86**, 1761
275 (2003).
- 276 [37] D. V Shalashilin, *J. Chem. Phys.* **132**, 244111 (2010).
- 277 [38] H. Tao, T. J. Martinez, H. Andersen, and P. H. Bucksbaum, *First Principles Molecular*
278 *Dynamics and Control of Photochemical Reactions*, Stanford University, 2011.
- 279 [39] D. V. Shalashilin, *Faraday Discuss.* **153**, 105 (2011).
- 280 [40] T. Northey, N. Zotev, and A. Kirrander, *J. Chem. Theory Comput.* **10**, 4911 (2014).

- 281 [41] U. Lorenz, K. B. Møller, and N. E. Henriksen, *Phys. Rev. A* **81**, 023422 (2010).
- 282 [42] N. E. Henriksen and K. B. Møller, *J. Phys. Chem. B* **112**, 558 (2008).
- 283 [43] K. Møller and N. Henriksen, in *Mol. Electron. Struct. Transit. Met. Complexes I*, edited
284 by D. M. P. Mingos, P. Day, and J. P. Dahl (Springer Berlin Heidelberg, Berlin,
285 Heidelberg, 2012), pp. 185–211.
- 286 [44] G. Dixit, O. Vendrell, and R. Santra, *Proc. Natl. Acad. Sci. U. S. A.* **109**, 11636 (2012).
- 287 [45] G. Dixit and R. Santra, *J. Chem. Phys.* **138**, 134311 (2013).
- 288 [46] Matlab, (2012).
- 289 [47] S. Adachi, M. Sato, and T. Suzuki, *J. Phys. Chem. Lett.* **6**, 343 (2015).

290

291 **ACKNOWLEDGEMENTS**

292 This research was carried out at the Linac Coherent Light Source (LCLS) at the SLAC
293 National Accelerator Laboratory. LCLS is an Office of Science User Facility operated for the
294 U.S. Department of Energy Office of Science by Stanford University. P.M.W. acknowledges
295 partial support by the National Science Foundation, grant number CBET-1336105. A.K., K.S.
296 and T.N. acknowledge grants FP7-PEOPLE-2013-CIG-NEWLIGHT (European Union) and
297 RPG-2013-365 (Leverhulme Trust), and helpful discussions with D. Shalashilin (Leeds).

298

299

300

301

302

303

304

305

306

307

308

309

310

311

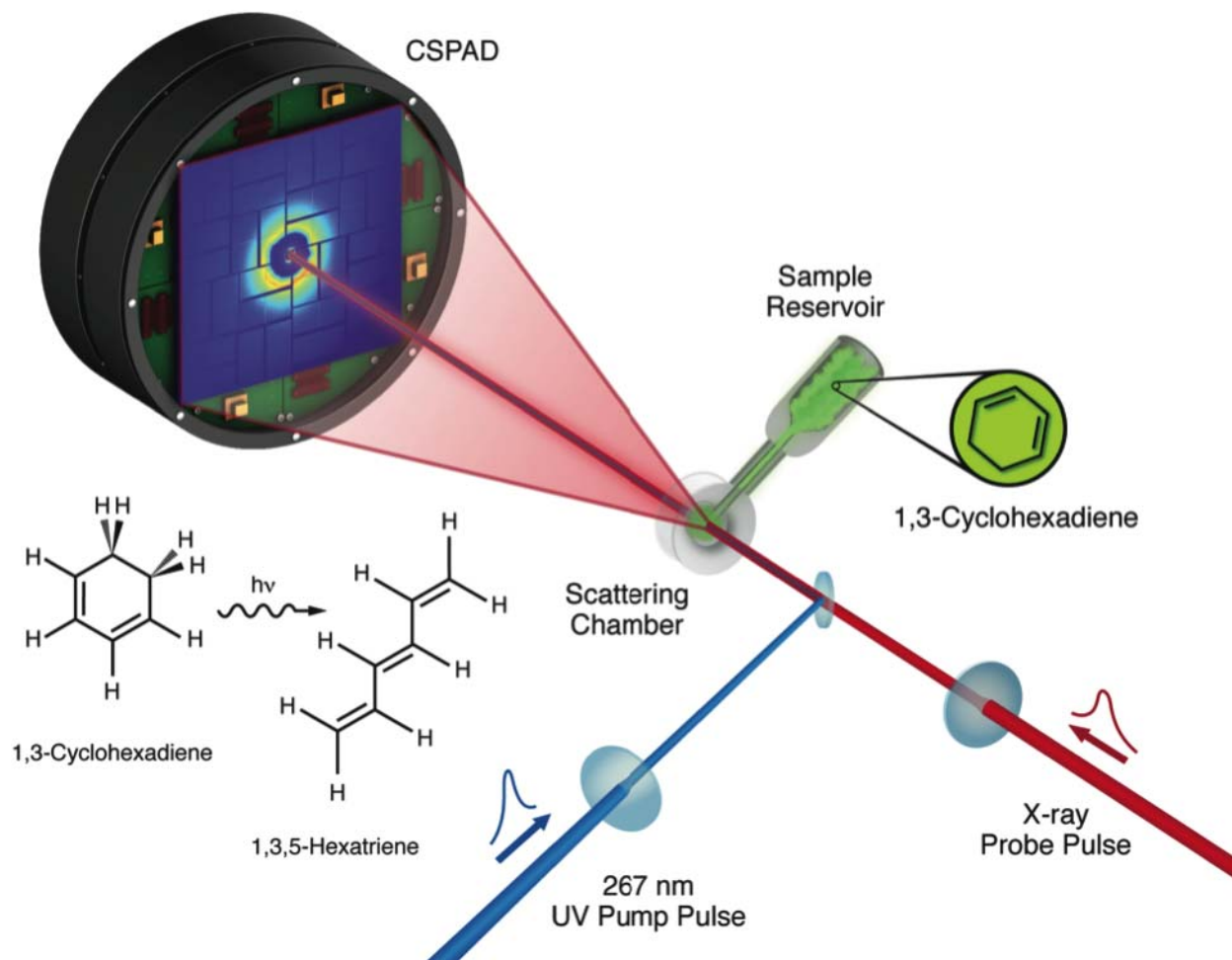
312 MAIN TEXT FIGURES & FIGURE CAPTIONS

313

314 **Figure 1.**

315

316



317

318

319 **Figure 1: (Color)** Experimental setup for ultrafast time resolved x-ray scattering studies.

320 Low pressure 1,3-cyclohexadiene vapor (green) is introduced into the scattering cell via a

321 needle valve from a room temperature sample reservoir. CHD is excited to the photoactive

322 state by the UV optical pump pulse (blue), inducing the chemical reaction that leads to

323 several conformers of 1,3,5-hexatriene. The reacting molecules are probed by diffracting

324 photons from an 8.3 keV x-ray pulse (red) that arrives with variable time delay relative the

325 pump pulse, onto a large area pixel array detector. The time delay between the optical and

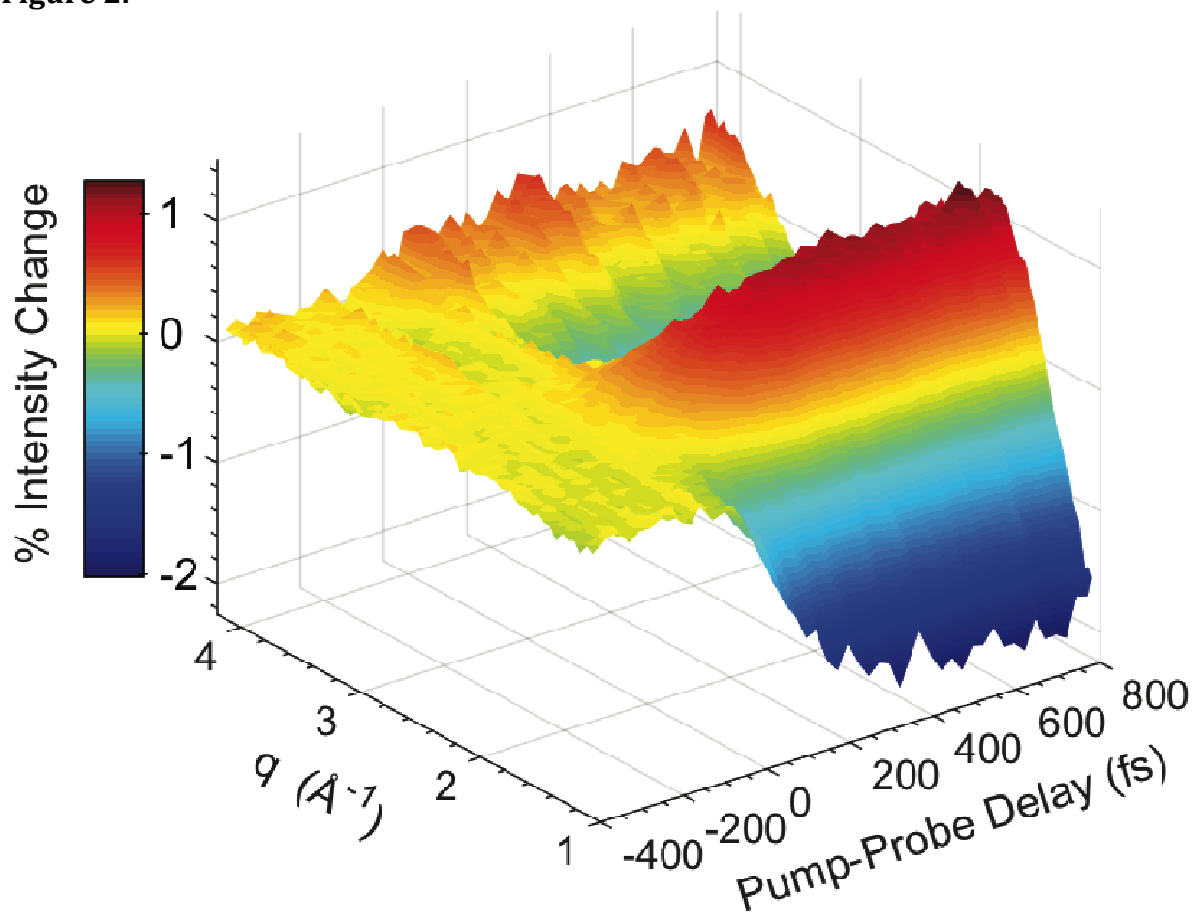
326 x-ray pulses are varied to obtain the complete molecular movie.

327

328

329

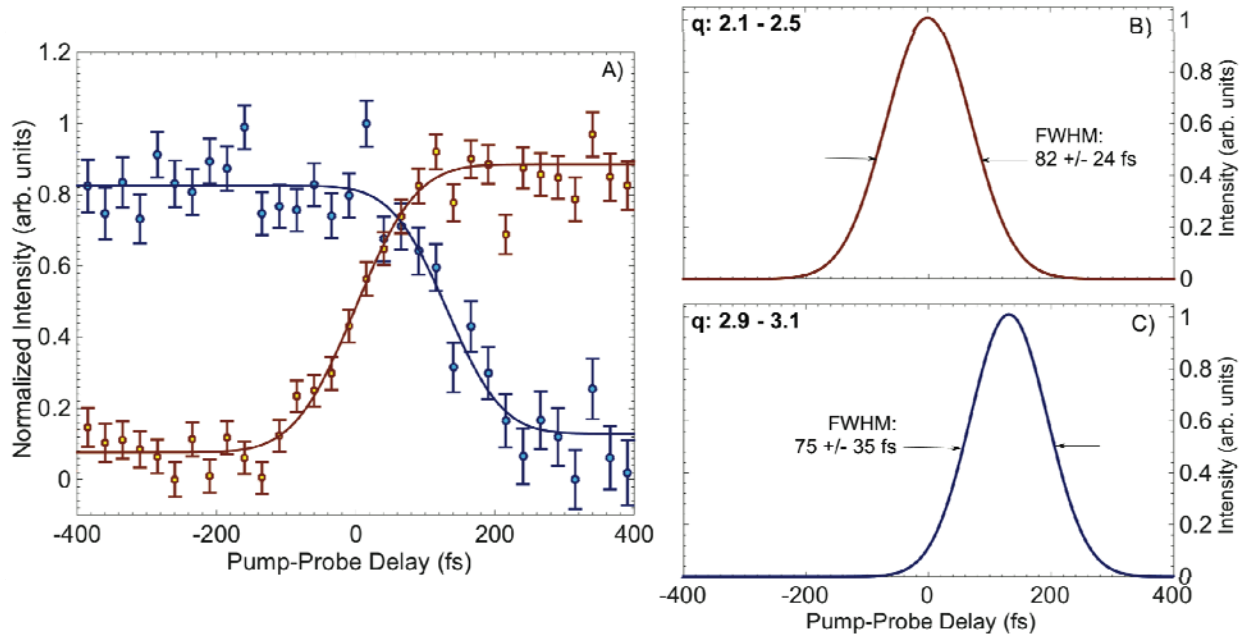
330 **Figure 2.**



331 **Figure 2: (Color)** The time-dependent pump-probe signal, defined as the percent
332 difference. The scattering patterns for positive delay times versus negative delay times
333 $(100 * ((\text{laser on-laser off}) / \text{laser off}))$, as a function of pump-probe delay time. The
334 scattering signals change on the order of 1% to 2% as indicated by the color bar.
335
336

337
338
339
340
341
342
343
344
345
346
347
348
349

350 **Figure 3.**
351

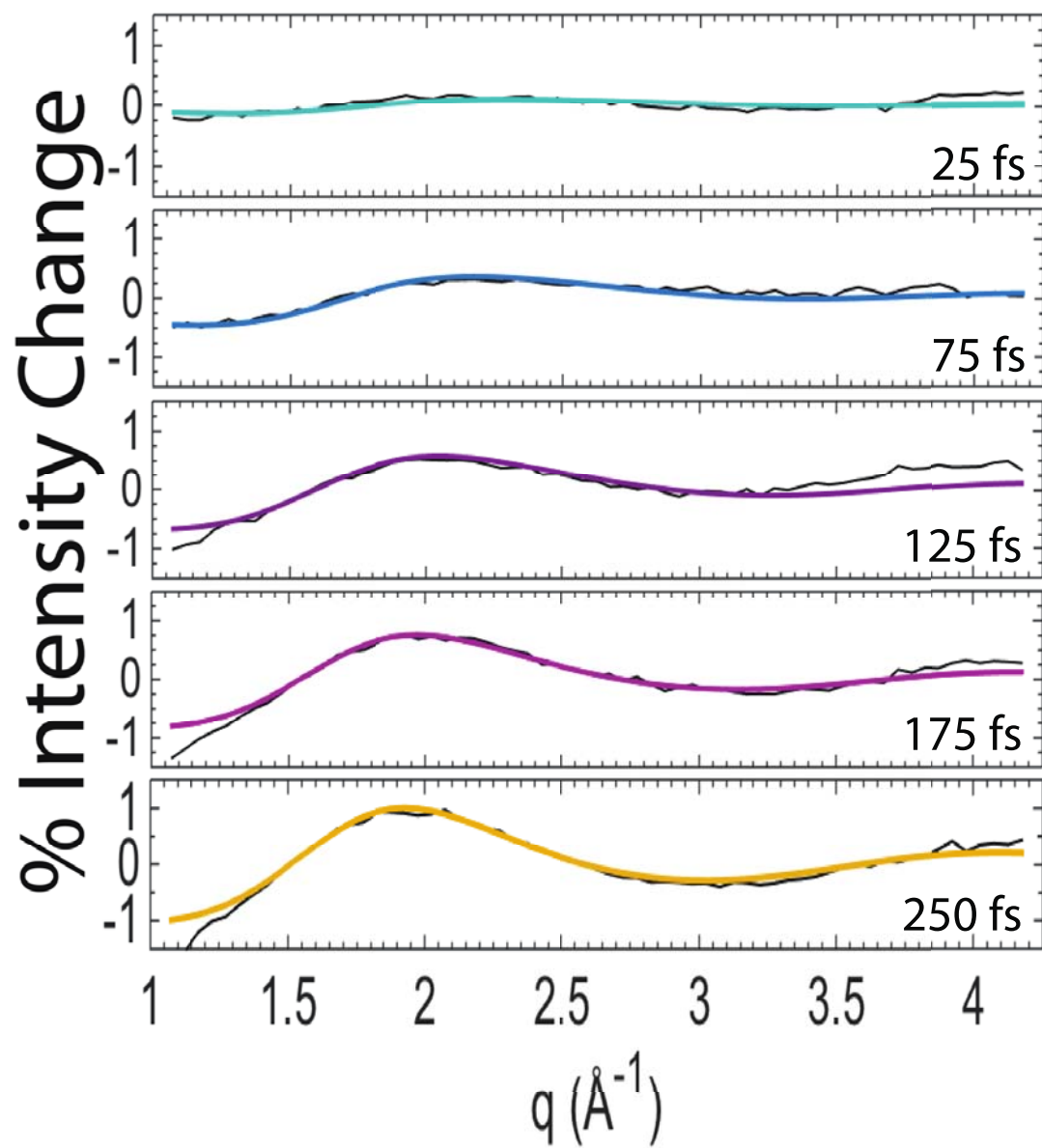


352
353

354 **Figure 3: (Color)** Time-dependent scattered signal intensities. **A)** Line traces of the
355 scattering signals at 2.1 – 2.5 Å (red squares) and 2.9 – 3.1 Å (blue circles), and fits (red and
356 blue lines, respectively). **B & C)** The derivatives of the fits show transients of 82 ± 24 and
357 75 ± 35 fs, respectively. Error bars for the fits in **A)** and the uncertainties in **B & C)** are
358 reported to 3σ calculated from the frame-to-frame shot noise from the CSPAD detector .
359

360
361
362
363
364
365
366
367
368
369
370
371
372
373
374
375

376 **Figure 4.**



377
378 **Figure 4: (Color)** Experimental (black lines) and computational (thick colored lines)
379 scattering signals for the first 250 fs of the ring-opening reaction of 1,3-cyclohexadiene.
380